

New limits on dark-matter WIMPs from the Heidelberg–Moscow experiment

L. Baudis, J. Hellmig, G. Heusser, H.V. Klapdor–Kleingrothaus*, S. Kolb, B. Majorovits, H. Päs, Y. Ramachers and H. Strecker

Max-Planck-Institut für Kernphysik, P.O.Box 10 39 80, D-69029 Heidelberg, Germany

V. Alexeev, A. Bakalyarov, A. Balysh, S.T. Belyaev*, V.I. Lebedev and S. Zhukov
Russian Science Centre Kurchatov Institute, 123 182 Moscow, Russia

New results after 0.69 kyr of measurement with an enriched ^{76}Ge detector of the Heidelberg–Moscow experiment with an active mass of 2.758 kg are presented. An energy threshold of 9 keV and a background level of 0.042 counts/(kg d keV) in the energy region between 15 keV and 40 keV was reached. The derived limits on the WIMP–nucleon cross section are the most stringent limits on spin-independent interactions obtained to date by using essentially raw data without background subtraction. *PACS number(s)*: 95.35.+d, 14.80.Ly

INTRODUCTION

The nature of dark matter in the Universe remains a challenging question. Even if new measurements will confirm that we live in a low Ω_{matter} universe ($\Omega_{\text{matter}} \sim 0.3\text{--}0.4$) [1,2] a considerable amount of nonbaryonic dark matter is needed. WIMPs (weakly interacting massive particles) are among the most discussed candidates [3], being well motivated from early universe physics [4] and supersymmetry [5].

WIMP detection experiments can decide whether WIMPs dominate the halo of our Galaxy. For this reason, considerable effort is made towards direct WIMP search experiments which look for energy depositions from elastic WIMP–nucleus scattering [6]. Germanium experiments designed for the search for neutrinoless double beta decay were among the first to set such kind of limits [7,8].

The Heidelberg–Moscow experiment gave the most stringent upper limits on spin-independent WIMP interactions [9] until recently. The present best limits on the WIMP–nucleon cross section come from the DAMA NaI Experiment [10]. The Heidelberg–Moscow experiment operates five enriched ^{76}Ge detectors with an active mass of 10.96 kg in the Gran Sasso Underground Laboratory. It is optimized for the search for the neutrinoless double beta decay of ^{76}Ge in the energy region of 2038 keV. For a detailed description of the experiment and latest results see [12].

In this paper we report on results from one of the enriched Ge detectors, which took data in a period of 0.249 years in a special configuration developed for low energy measurements. A lower energy threshold and a smaller background counting rate has been achieved with the same detector as used in 1994 [9], mainly due to the lower cosmogenic activities in the Ge crystal and in the surrounding copper after four years without activation.

EXPERIMENTAL SETUP

The utilized detector is a coaxial, intrinsic p-type HPGe detector with an active mass of 2.758 kg. The enrichment in ^{76}Ge is 86%. The sensitivity to spin-dependent interactions becomes negligible, since ^{73}Ge , the only stable Ge isotope with nonzero spin, is deenriched to 0.12% (7.8% for natural Ge). The detector has been in the Gran Sasso Underground Laboratory since September 1991; a detailed description of its background can be found in [12].

The data acquisition system allows an event-by-event sampling and pulse shape measurements. The energy output of the preamplifier is divided and amplified with two different shaping time constants, 2 μs and 4 μs . The fast 2 μs signal serves as a stop signal for the 250 MHz flash analogue to digital converter (FADC) which records the pulse shape of each interaction. The best energy resolution and thus lowest energy threshold is obtained with the 4 μs shaped signal. A third branch of the energy output is shaped with 3 μs and amplified to record events up to 8 MeV in order to identify radioactive impurities contributing to the background. The spectra are measured with 13bit ADCs, which also release the trigger for an event by a peak detect signal. Further triggers are vetoed until the complete event information, including the pulse shape, has been recorded. To record the pulse shape (for details see [13]) the timing output of the preamplifier is divided into four branches, each signal being integrated and differentiated in filtering amplifiers (TFAs) with different time constants. The TFAs are used since the charge current is integrated within the preamplifier. The signals are amplified to record low as well as high-energetic pulses.

DATA ANALYSIS

An energy threshold of 9 keV has been reached. This rather high value is due to the large detector size and

a 50 cm distance between FET and detector. Both effects lead to a higher system capacitance and thus to an enhancement of the baseline noise.

We calibrate the detector with a standard ^{152}Eu - ^{228}Th source. The energy resolution at 727 keV is (2.37 ± 0.01) keV. In order to determine the energy resolution at 0 keV the dependence of the full width at half maximum (FWHM) on the energy is approximated with an empirical function $y = \sqrt{a + bx + cx^2}$ (y = resolution, x = energy) in a χ^2 fit. The best fit ($\chi^2/\text{DOF} = 0.09$) is obtained for the parameters $a = 3.8$, $b = 2.2 \times 10^{-3}$, $c = 5 \times 10^{-7}$. The zero energy resolution is (2 ± 0.01) keV.

To determine the energy threshold, a reliable energy calibration at low energies is required. The lowest energetic line observed in the detector was at 74.97 keV (K_α line of ^{208}Pb). This is due to the rather thick copper shield of the crystal (2 mm) which absorbs all low energy γ lines. Thus an extrapolation of the energy calibration to low energies is needed, which induces an error of (1–2) keV. Another possibility is to use a precision pulser in order to determine the channel of the energy spectrum which corresponds to zero voltage pulser output. Since the slope of the energy calibration is independent of the intercept and can be determined with a calibration source, this method yields an accurate value for the intercept of the calibration. The same method to determine the offset of the calibration is also used by [9] and [14]. The pulser calibration reduces the extrapolated 9 keV threshold systematically by (1–2) keV. In order to give conservative results, we use the 9 keV threshold for data analysis.

In Fig. the energy deposition as a function of time is plotted. Accumulation of events (bursts) with energy depositions up to 30 keV can be seen. They are irregularly distributed in time with counting rate excesses up to a factor of five. These events can be generated by microphonics (small changes in the detector capacitance due to changes in temperature or mechanical vibrations) or by a raised electronic noise on the baseline. Although rare, they lead to an enhancement of the count rate in the low energy region. A possibility to deal with microphonics would be to exclude the few days with an enhanced count rate from the sum spectrum like in [7]. This would lead, however, to unwanted measuring time losses. Another time filtering method is applied in the following.

The complete measuring time is divided into 30-minute intervals and the probability for N events to occur in one time interval is computed for energy depositions between 9–850 keV. In the histogram in Fig. the physical events are Poisson distributed. The mean value of the distribution is (2.65 ± 0.06) events/30 min and $\sigma = (1.67 \pm 0.05)$. The cut is set at the value $N = 2.65 + 3\sigma \approx 8$. With this cut less than 0.01% of the undisturbed 30 minutes intervals are rejected. The initial exposure of the measurement was 0.7 kg yr, after the time cut the exposure is 0.69 kg yr. In this way, more than 98% of the initial data are used. A similar method to reduce the microphonic

noise in the low energy region was also applied by [9].

Another way to reject microphonic events would be to analyze the recorded pulse shapes of each event. In a former experiment we showed [13] that pulse shapes of nuclear recoil and γ interactions are indistinguishable within the timing resolution of Ge detectors. Thus a reduction of γ -ray background based on pulse shape discrimination (PSD) is not possible. Consequently γ sources can be employed to calibrate a PSD method against microphonics, which was shown to reveal a different pattern in the pulse shape. Since such a pulse shape analysing method is still under development, we use only the Poisson–time–cut method in this paper.

Figure shows the sum spectrum after the time cut. The background counting rate in the energy region between 9 keV and 30 keV is 0.081 cts/(kg d keV) [between 15 keV and 40 keV: 0.042 cts/(kg d keV)]. This is about a factor of two better than the background level reached by [9] with the same Ge detector. Table I gives the number of counts per 1 keV bin for the energy region between (9–50) keV. The dominating background contribution in the low–energy region from the U/Th natural decay chain can be identified in Fig. via the 352 keV and 609 keV lines (the continuous beta spectrum from ^{210}Bi originates from this chain).

DARK MATTER LIMITS

The evaluation for dark matter limits on the WIMP–nucleon cross section $\sigma_{\text{scalar}}^{\text{W-N}}$ follows the conservative assumption that the whole experimental spectrum consists of WIMP events. Consequently, excess events from calculated WIMP spectra above the experimental spectrum in any energy region with a minimum width of the energy resolution of the detector are forbidden (to a given confidence limit).

The parameters used in the calculation of expected WIMP spectra are summarized in Table II. We use formulas given in the extensive reviews [15,16] for a truncated Maxwell velocity distribution in an isothermal WIMP–halo model (truncation at the escape velocity, compare also [17]).

Since ^{76}Ge is a spin zero nucleus, we give cross section limits for WIMP–nucleon scalar interactions only. For these, we used the Bessel form factor (see [16] and references therein) for the parametrization of coherence loss, adopting a skin thickness of 1 fm.

Another correction which has to be applied for a semiconductor ionization detector is the ionization efficiency. There exist analytic expressions [6] for this efficiency, especially for germanium detectors and multiple experimental results measuring this quantity (see [13] and references therein). According to our measurements [13] we give a simple relation between visible energies and recoil energies: $E_{\text{vis}} = 0.14 E_{\text{recoil}}^{1.19}$. This relation has been checked for consistency with the relation from [6] in the

relevant low energy region above our threshold.

After calculating the WIMP spectrum for a given WIMP mass, the scalar cross section is the only free parameter which is then used to fit the expected to the measured spectrum (see Fig.) using a one-parameter maximum-likelihood fit algorithm. According to the underlying hypothesis (see above) we check during the fit for excess events above the experimental spectrum (for a one-sided 90% C.L.) using a sliding, variable energy window. The minimum width of this energy window is 5 keV, corresponding to 2.5 times the FWHM of the detector (6σ width). The minimum of cross section values obtained via these multiple fits of the expected to the measured spectrum gives the limit. Figure shows a comparison between the measured spectrum and the calculated WIMP spectrum for a 100 GeV WIMP mass. The solid curve represents the fitted WIMP spectrum using a minimum width of 5 keV for the energy window. The minimum is found in the energy region between 15 keV and 20 keV. The dashed line is the result of the fit if the energy window width equals the full spectrum width. It is easy to see that in this case the obtained limit would be much too conservative, leading to a loss of the information one gets from the measured spectrum.

CONCLUSIONS

The new upper limit exclusion plot in the $\sigma_{\text{scalar}}^{\text{W-N}}$ versus M_{WIMP} plane is shown in Fig. . Since we do not use any background subtraction in our analysis, we consider our limit to be conservative. We are now sensitive to WIMP masses greater than 13 GeV and to cross sections as low as 1.12×10^{-5} pb (for $\rho = 0.3$ GeV/cm³).

At the same time we start to enter the region (evidence-contour) allowed with 90% C.L. if the preliminary analysis of 4549 kg days of data by the DAMA NaI Experiment [18] are interpreted as an evidence for an annual modulation effect due to a spin independent coupled WIMP.

Should the effect be confirmed with much higher statistics (20 000 kg days are now being analyzed by the DAMA Collaboration [19]) it could become crucial to test the region using a different detector technique and a different target material.

Also shown in the figure are recent limits from the CDMS Experiment [20], from the DAMA Experiment [10], as well as expectations for new dark matter experiments like CDMS [20], HDMS [21] and for our recently proposed experiment GENIUS [22]. Not shown is the limit from the UKDM Experiment [11] which lies somewhere between the two germanium limits.

After a measuring period of 0.69 kg yr with one of the enriched germanium detectors of the Heidelberg-Moscow experiment, the background level decreased to 0.0419 counts/(kg d keV) in the low energy region. The WIMP-nucleon cross section limits for spin-independent inter-

actions are the most stringent limits obtained so far by using essentially raw data without background subtraction.

An improvement in sensitivity could be reached after a longer measuring period. Higher statistics would allow the identification of the various radioactive background sources and would open the possibility of a quantitative and model-independent background description via a Monte Carlo simulation. Such a background model has already been established for three of the enriched Ge detectors in the Heidelberg-Moscow experiment and has been successfully applied in the evaluation of the $2\nu\beta\beta$ decay [12]. A subtraction of background in the low energy region in the form of a phenomenological straight line based on a quantitative background model for the full energy region (9 keV – 8 MeV) would lead to a further improvement in sensitivity. Background subtractions for dark matter evaluations of Ge experiments were already applied by [23].

Another way to reject radioactive background originating from multiple scattered photons would be an active shielding in the immediate vicinity of the measuring crystal. This method is applied in our new dark matter search experiment, HDMS (Heidelberg Dark Matter Search) [21]. HDMS is situated in the Gran Sasso Underground Laboratory and started operation this year.

ACKNOWLEDGMENTS

The Heidelberg-Moscow experiment was supported by the Bundesministerium für Forschung und Technologie der Bundesrepublik Deutschland, the State Committee of Atomic Energy of Russia and the Istituto Nazionale di Fisica Nucleare of Italy. L.B. was supported by the Graduiertenkolleg of the University of Heidelberg.

* Spokesmen of the collaboration

- [1] S. Perlmutter *et al.*, Nature (London) **391**, 51 (1998).
- [2] A.G. Riess *et al.*, astro-ph/9805201.
- [3] G. Jungman, M. Kamionkowski, and K. Griest, Phys. Rep. **267**, 195 (1996).
- [4] E. W. Kolb and M. S. Turner, *The Early Universe* (Addison-Wesley, Reading MA, 1994).
- [5] H. E. Haber and G. L. Kane, Phys. Rep. **117**, 75 (1985).
- [6] P.F. Smith and J.D. Lewin, Phys. Rep. **187**, 203 (1990).
- [7] S.P. Ahlen *et al.*, Phys. Lett. B **195**, 603 (1987)
- [8] D.O. Caldwell *et al.*, Phys. Rev. Lett. **61**, 510 (1988).
- [9] Heidelberg-Moscow Collaboration, Phys. Lett. B **336**, 141 (1994).
- [10] R. Bernabei *et al.*, Phys. Lett. **389**, 757 (1997).
- [11] P.F. Smith *et al.*, Phys. Lett. B **379**, 299 (1996).

- [12] Heidelberg–Moscow Collaboration, M. Günther *et al.* Phys. Rev. D **55**, 54 (1997) and L. Baudis *et al.* Phys. Lett. B **407**, 219 (1997).
- [13] L. Baudis *et al.*, NIMA 418/2-3 348-354 (1998).
- [14] D. Reusser *et al.*, Phys. Lett. B **255**, 143 (1991).
- [15] R. Bernabei, Riv. Nuovo Cimento **18**, 1 (1995).
- [16] J.D. Lewin and P.F. Smith, Astropart. Phys. **6**, 87 (1997).
- [17] K. Freese, J. Frieman, and A. Gould, Phys. Rev. D **37**, 3388 (1988).
- [18] R. Bernabei *et al.*, Nucl. Phys. B (Proc. Suppl)**70**, 79 (1998).
- [19] R. Bernabei, in *Proceedings of the Second International Conference on Dark Matter in Astro and Particle Physics*, Heidelberg, Germany 1998, edited by H.V. Klapdor–Kleingrothaus and L. Baudis (IOP, Bristol, 1999).
- [20] CDMS Collaboration, D. S. Akerib *et al.*, Nucl. Phys. B (Proc. Suppl) **70** (Proc. Suppl) 64 (1998).
- [21] L. Baudis *et al.*, Nucl. Instrum. Methods A **385**, 265 (1997).
- [22] H.V. Klapdor–Kleingrothaus, in *Proceedings of the First International Conference on Particle Physics Beyond the Standard Model*, Castle Ringberg, Germany, 8–14 June 1997, edited by H.V. Klapdor–Kleingrothaus and H. Päs, (IOP, Bristol, 1998), H.V. Klapdor–Kleingrothaus, J. Hellmig and M. Hirsch, J. Phys. G **24**, 483–516 (1998), L. Baudis *et al.*, submitted to NIMA.
- [23] E. Garcia *et al.*, Phys. Rev. D **51**, 1458 (1995).
- [24] V. Bednyakov *et al.*, Z. Phys. A **357** 339 (1997).

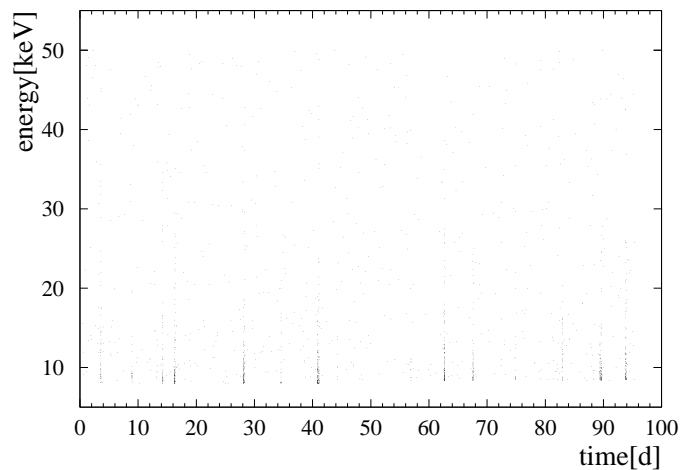


FIG. 1. Energy spectrum as a function of time for the enriched ^{76}Ge detector for the whole measurement period. Irregular bursts up to 30 keV can be seen.

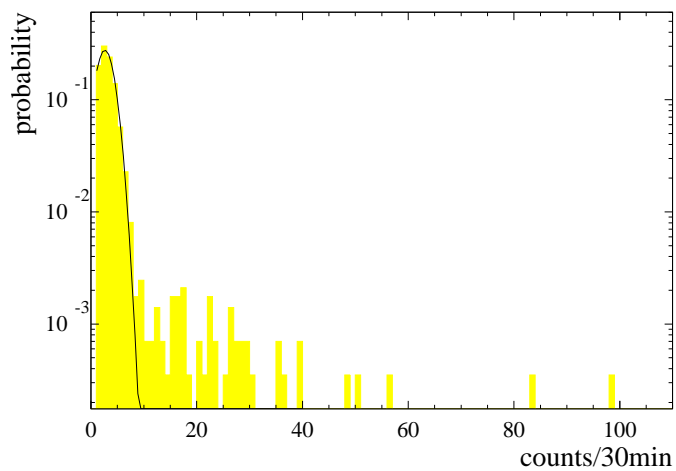


FIG. 2. Distribution of the number of events with energies between 9 keV and 850 keV per 30-minute interval. The solid curve represents the Poisson fit to the data.

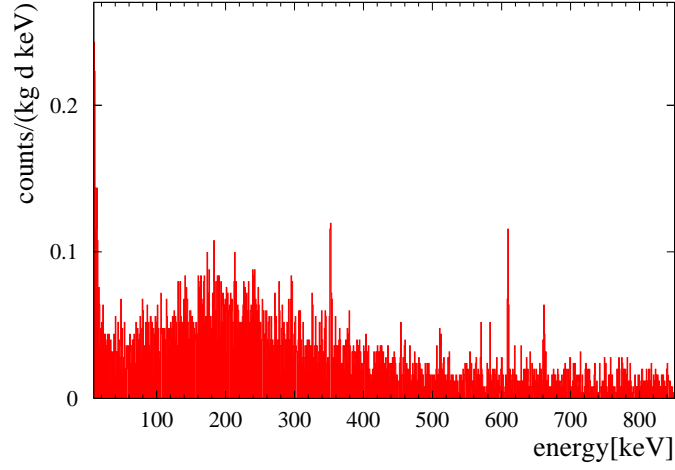


FIG. 3. Full recorded sum spectrum with lifetime 0.69 kg yr. Peaks from the ^{238}U chain can be identified. A ^{137}Cs peak slowly appears at 662 keV. All structures at low energies are fluctuations so far and therefore not identifiable.

TABLE I. Number of counts per 1 keV energy bin after 250.836 kg d.

Bin [keV]	Counts [1/keV]	Bin [keV]	Counts [1/keV]
9-10	61	30-31	10
10-11	56	31-32	11
11-12	36	32-33	2
12-13	29	33-34	10
13-14	36	34-35	7
14-15	27	35-36	8
15-16	16	36-37	8
16-17	19	37-38	7
17-18	16	38-39	11
18-19	9	39-40	8
19-20	12	40-41	14
20-21	13	41-42	4
21-22	10	42-43	8
22-23	16	43-44	6
23-24	11	44-45	13
24-25	8	45-46	10
25-26	11	46-47	5
26-27	9	47-48	7
27-28	9	48-49	17
28-29	10	49-50	9
29-30	11	50-51	12

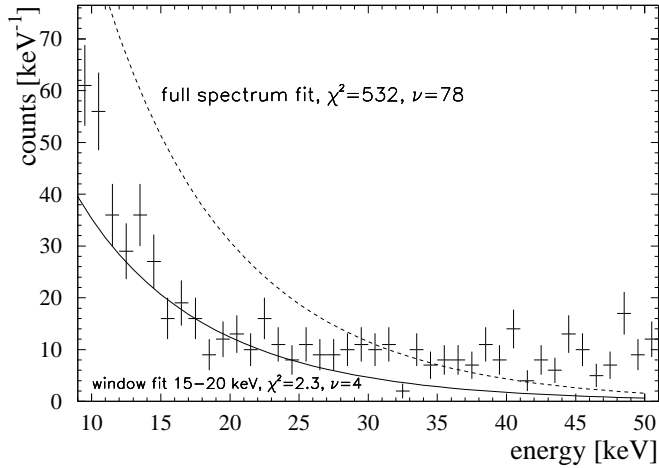


FIG. 4. Comparison of the measured low energy spectrum (shown from threshold to 50 keV) from the enriched ^{76}Ge Detector and calculated WIMP spectra for a 100 GeV WIMP, already fitted for the allowed cross section $\sigma_{\text{scalar}}^{\text{W-N}}$. The solid curve shows the result from the sliding-window fit (see text). The dashed curve would result for a full WIMP-spectrum fit to the data, yielding too conservative limits.

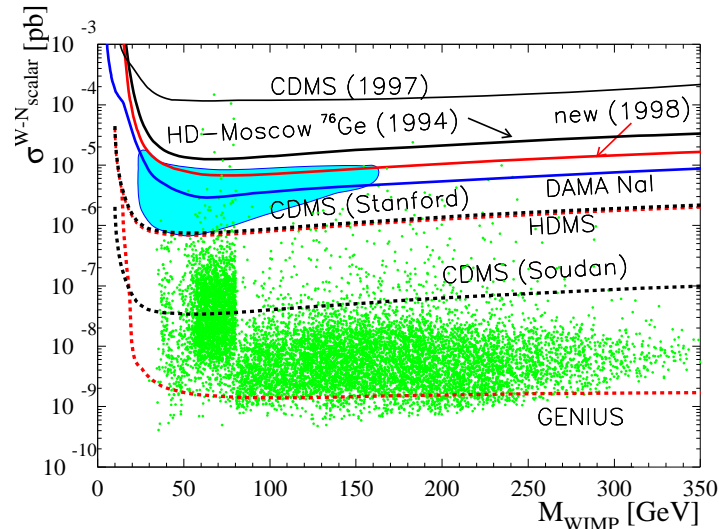


FIG. 5. Comparison of already achieved WIMP-nucleon scalar cross section limits (solid lines): the Heidelberg-Moscow ^{76}Ge [9], the recent CDMS nat. Ge [20] and the new DAMA NaI result [10], including their evidence contour [18], in pb for scalar interactions as function of the WIMP mass in GeV and of possible results from upcoming experiments (dashed lines for HDMS [21], CDMS (at different locations) and GENIUS [22]). These experimental limits are also compared to expectations (scatter plot) for WIMP neutralinos calculated in the MSSM framework with non-universal scalar mass unification [24] (all curves and dots scaled for $\rho = 0.5 \text{ GeV}/\text{cm}^3$ for comparison of published data).

TABLE II. List of parameters used for calculating WIMP spectra.

Parameter	Value
WIMP velocity distribution	270 km/s
Escape velocity	580 km/s
Earth velocity	245 km/s
WIMP local density	0.3 GeV/cm ³
enriched ⁷⁶ Ge mass	75.14 g/mol